Dark matter constraints from Fermi-LAT Inner Galaxy measurements

M.A. Sánchez-Conde (KIPAC/SLAC), G.A. Gómez-Vargas, A. Morselli on behalf of the Fermi-LAT Collaboration,
D.G. Cerdeno, J. Huh, A. Klypin, Y. Mambrini, C. Munoz, M. Peiro, F. Prada

We have obtained constraints on the parameter space of generic dark matter candidates performing an analysis of inner regions of the Milky Way, where the gamma-ray flux produced by dark matter annihilation is expected to be maximized. The analysis is conservative and simply requires that the expected dark matter signal does not exceed the observed gamma-ray emission by the Fermi-LAT in an optimized region around the Galactic Center.

Gamma-ray annihilation flux

Two main contributions in the Galactic Halo: **prompt** photons and photons induced via Inverse Compton Scattering (**ICS**).

Prompt:

$$\left(\frac{d\Phi_\gamma}{dE_\gamma}\right)_{prompt} = \sum_i \frac{dN_\gamma^i}{dE_\gamma} \frac{\langle\sigma_i v\rangle}{8\pi m_{DM}^2} \bar{J}(\Delta\Omega)\Delta\Omega$$

Particle physics | Astrophysics

i : annihilation channel
dN/dEγ : differential γ-ray yield
<σv> : averaged cross section
m_{DM} : DM mass

Line-of-sight integral of the squared DM density, i.e. *J-factor*:

$$\bar{J}(\Delta\Omega) \equiv \frac{1}{\Delta\Omega}\int d\Omega \int_{l.o.s.} \rho^2(r(l,\Psi))\, dl$$

ICS:

- Numerical calculation of galactic cosmic-rays diffusion-loss.
- Three different diffusion models: MIN, MED, MAX [1].
- ICS significant for leptonic channels; can be dominant over prompt for heavy DM in the energy range considered.

Dark matter density profiles

We use three well motivated profiles whose parameters (summarized in Table I) have been constrained from Milky Way observational data [2,3]. The **effect of baryons** on the NFW profile leads to the adiabatically compressed ***NFW$_c$***, which yields much higher annihilation fluxes, see Fig.1. Note, however, that the exact role of baryons is not fully understood yet and might act in the opposite direction.

$$\rho(r) = \frac{\rho_s}{\left(\frac{r}{r_s}\right)^\gamma \left[1+\left(\frac{r}{r_s}\right)^\alpha\right]^{\frac{\beta-\gamma}{\alpha}}} \qquad \rho_{\rm Ein}(r) = \rho_s \exp\left\{-\frac{2}{\alpha}\left[\left(\frac{r}{r_s}\right)^\alpha - 1\right]\right\}$$

Table I: DM density profile parameters used in this work.

Profile	α	β	γ	ρ_s [GeV cm^{-3}]	r_s [kpc]
Einasto	0.22	--	--	0.08	19.7
NFW	1	3	1	0.21	23.8
NFW$_c$	0.76	3.3	1.37	0.35	18.5

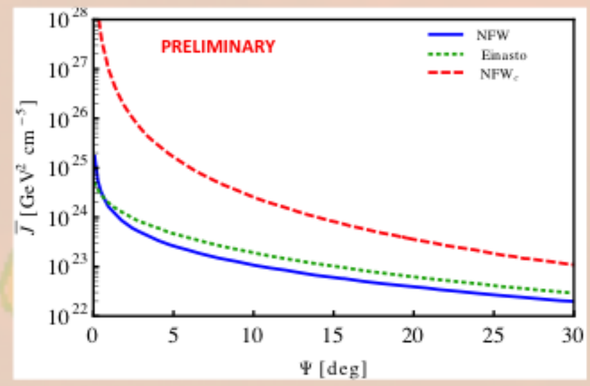

Figure 1: J-factor as a function of Ψ, for the DM density profles given in Table I: NFW, NFWc and Einasto.

Regions of Interest (ROIs) and Data Analysis

Data Analysis

- Fermi-LAT data from 08/08 to 06/12
- Energy range: 1-100 GeV
- Class events: P7V6 ultraclean front
- 30 deg around the GC
- 0.2 deg/pixel resolution flux maps

ROIs optimization

We choose the ROIs driven by a signal-to-noise optimization:

- ***Signal***: J-factor maps for every DM density profile.
- ***Noise***: Square root of the photon flux map.

ROI's optimal parameters are those that make S/N the largest for every DM density profile, see Table II and Figure 2.

Figure 2: Optimized ROIs for NFW (left) and NFW$_c$ (right). Einasto ROI, not shown here, is very similar to NFW. An schematic view of our choice of ROI is also shown below, with gray regions corresponding to masked regions.

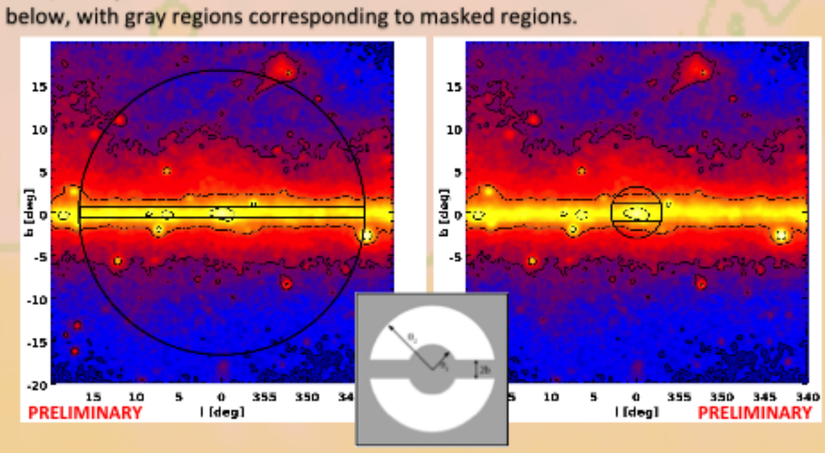

Table II: Values of the parameters that define the best ROI in every case. J-factors and Fermi fluxes are also given.

Profile	θ_1 [deg]	θ_2 [deg]	$\lvert b\rvert$ [deg]	$\Delta\Omega$ [sr]	$\bar{J}(\Delta\Omega)\,\Delta\Omega$ [$\times 10^{22}$ GeV^2 cm^{-5} sr]	Flux (1 – 100 GeV) [$\times 10^{-7}$ cm^{-2}s^{-1}]
Einasto	0.7	15.6	0.7	0.217	5.1	31.4 ± 0.3
NFW	0.6	16.7	0.6	0.253	3.3	38.0 ± 0.3
NFW$_c$	1.0	3.0	1.0	0.005	86.8	2.2 ± 0.1

Results (Preliminary)

By comparing the inclusive energy spectrum extracted from the data for every ROI (shown in Fig.3) and the J-factors in Table II, we set DM constraints only requesting that the DM-induced gamma-ray emission *does not overshoot* the flux measurement at ***3σ*** level.

Profile	$\bar{J}(\Delta\Omega)\,\Delta\Omega$ [$\times 10^{22}$ GeV^2 cm^{-5} sr]
Einasto	5.1
NFW	3.3
NFW$_c$	86.8

VS.

Figure 3: Inclusive energy spectrum extracted from Fermi-LAT data for the ROIs in Table II. Vertical error bars correspond to statistical errors (from the square root of number counts), while boxes represent systematic erros in Fermi-LAT effective area.

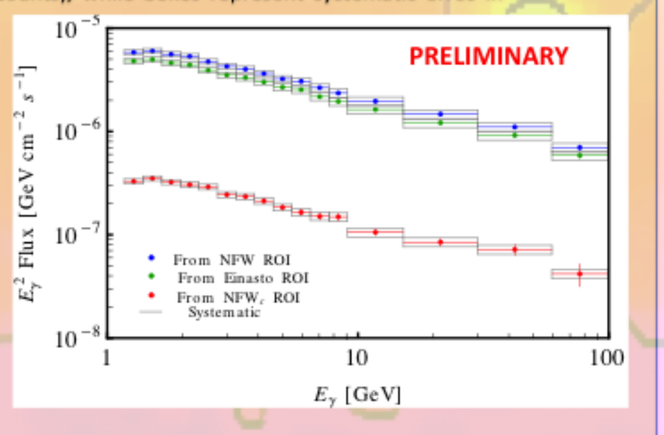

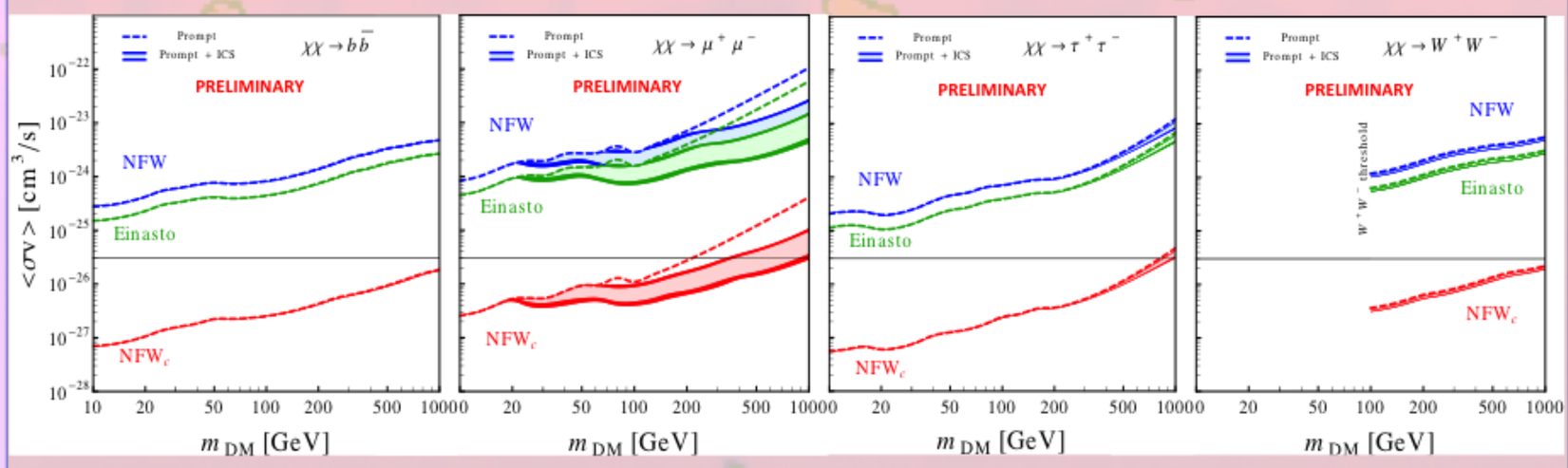

Figure 4: 3σ upper limits on the annihilation cross-section of models in which DM annihilates into bb, $\mu^+\mu^-$, $\tau^+\tau^-$, W^+W^- (from left to right), for the three DM density profiles in Table I. Upper limits without including ICS are also given as dashed curves (prompt) for comparison. The uncertainty in the diffusion model is shown as the thickness of the solid curves (from top to bottom: MIN, MED, MAX) while the lighter shaded regions represent the impact of the different strengths of the Galactic magnetic field with lower(higher) values of the cross-section corresponding to 1 μG (10 μG) at Earth. The horizontal line corresponds to the expected value of the thermal cross-section for a generic WIMP candidate.

Conclusions

For NFW and Einasto DM profiles we find upper limits on the annihilation cross-section comparable to the ones previously reported by the Fermi-LAT collaboration, after a similar analysis of the Galactic halo without modeling of the astrophysical background [4]. When adiabatic contraction of the DM due to the infall of baryons is taken into account, the limits are more than 2 orders of magnitude stronger. In particular, for bb, $\tau^+\tau^-$, W^+W^- annihilation channels, the thermal cross-section is excluded for a DM mass < 1 TeV. For the m^+m^- channel, where the ICS effect is important, depending on the modelization of the galactic magnetic field, the thermal cross-section is excluded for a mass smaller than about 300 GeV to 1 TeV.

References

[1] T. Delahaye et al., 2008, PRD, 77,063527
[2] F. Prada et al., 2004, PRL, 93, 241301
[3] Catena & Ullio, 2010, JCAP, 08, 004
[4] M. Ackermann et al, 2012, arXiv:1205.6474